Nonlinear Effect of GdnHCl on Hydration Dynamics of Proteins: A H−1 Magnetic Relaxation Dispersion Study

ARTICLE *in* THE JOURNAL OF PHYSICAL CHEMISTRY B · MAY 2009

Impact Factor: 3.3 · DOI: 10.1021/jp8114836 · Source: PubMed

4 AUTHORS, INCLUDING:

Trivikram Rao Molugu
The University of Arizona
12 PUBLICATIONS **35** CITATIONS

SEE PROFILE

Nonlinear Effect of GdnHCl on Hydration Dynamics of Proteins: A ^{1}H Magnetic Relaxation Dispersion Study

M. Trivikram Rao,[†] Abani K. Bhuyan,*[,‡] K. Venu,[†] and V. S. S. Sastry*[,†]

Schools of Physics and Chemistry, University of Hyderabad, Hyderabad 500046, India

Received: December 30, 2008; Revised Manuscript Received: March 7, 2009

Proton magnetic relaxation dispersion investigations with aqueous solutions of lysozyme and bovine serum albumin (BSA) in the 0−5 M range of guanidine hydrochloride (GdnHCl), pH 4.4, 27 °C, were taken up with the objective of examining the hydration dynamics of internal cavity waters as the protein is held under increasingly destabilizing conditions. Field cycling NMR and conventional pulsed NMR techniques were employed to cover a frequency range of 100 kHz to 50 MHz. Analyses of dispersion profiles at different concentrations of GdnHCl were carried out considering the contributions from internal and surface waters. The denaturant-dependent variation of internal water contribution indicates that the reorientational disorder of internal waters decreases with increments of the denaturant up to its subdenaturing limit. For both proteins, the variation of effective correlation time with GdnHCl apparently shows a marginal shrink in hydrodynamic volumes under the subdenaturing condition. These results suggest that subdenaturing amounts of GdnHCl restrict the motional freedom of the internal waters, and can have considerable influence on the surface hydration. On increasing the denaturant concentration further, the dispersion amplitude drops sharply, indicating that the chaotropic action of the denaturant now runs over its own cavity water-ordering effect operative in the subdenaturing limit. The results are fundamentally important for the understanding of the susceptibility of protein structure and hydration to denaturants.

1. Introduction

Water molecules in the protein−water system are generally grouped into three classes, bulk water, surface water, and internal cavity water, but what role each class of water plays in the folding and maintenance of protein structure is poorly understood. Since experimental investigations of protein folding and stability almost exclusively rely on the use of chemical denaturants like urea and GdnHCl, studies of the effect of denaturants on the structure and dynamics of each class of water molecules are imperative. Investigations of the effect of urea on bulk water structure began four decades ago.[1] NMR studies of aqueous urea solutions appeared to show that the denaturant exerts its effect by shifting the $(H_2O)_{bulky} \leftrightarrows (H_2O)_{dense}$ equilibrium toward the dense phase. The model and its implication for protein structure and folding has been controversial, though,[2] even at the present.[3] Relatively recent experimental studies on the hydration dynamics of the surface layer of water have shed some light on the role of surface-bound water in protein stability and folding,[4] and enzyme activity.[5] The hydration time for the surface-bound water molecules is apparently a determinant of protein stability.[4] Computer simulations show that the surface-bound water, whose density is substantially more than that of bulk water,[6] may cause polypeptide collapse and mediate the formation of tertiary structure.[7]

However, studies on the dynamical behavior of the internally trapped water and their possible role in the folding and stability of proteins have been scarce, although they have been implicated in the functional events of binding, recognition, and catalysis.[8] They are fewer in number, and their time-averaged position in the cavities and in some cases the interactions with the backbone and side chains of proteins are recognized in X-ray structures.[8,9] Cavity waters are distinct from surface-bound waters in terms of the residence time or hydration time: ∼10 ns to 1 ms for the former and tens of picoseconds to a few hundred picoseconds for the latter.[10−12]

Direct probing of cavity water hydration under varying conditions of denaturant may provide important information about their response to structural changes during protein unfolding. With this rationale, we have initiated a series of studies using aqueous solutions of proteins each held under varying conditions of denaturant-induced stability. This article reports on the influence of GdnHCl on the hydration dynamics of lysozyme and bovine serum albumin (BSA) by the use of proton magnetic relaxation dispersion (PMRD), a tool explored in relatively more detail during the recent years.[13−15] The magnetic relaxation dispersion method has actually been used to study urea and GdnHCl-induced protein unfolding,[14,16,17] although the specific effect of protein stabilization by subdenaturing concentrations of the denaturants has not been investigated. The two proteins chosen for the study here are paradigms for structural, functional, and folding studies[18−27] and find extensive use in biochemistry. Both lysozyme and BSA have been used in earlier PMRD measurements.[13,28,29] We analyze the dispersion amplitude in the relaxation spectral density generated by recording the dependence of the longitudinal relaxation rate of water protons on the Larmor frequency. For both proteins, the dispersion amplitude increases as the solvent composition is altered by the addition of small amounts of GdnHCl but decreases under strongly destabilizing conditions. Analyses in terms of the generalized order parameter representing internal dynamics of water molecules with respect to the

* Corresponding authors. E-mail: akbsc@uohyd.ernet.in (A.K.B.); vssssp@uohyd.ernet.in (V.S.S.S.).
[†] School of Physics.
[‡] School of Chemistry.

10.1021/jp8114836 CCC: $40.75
Published on Web 04/23/2009

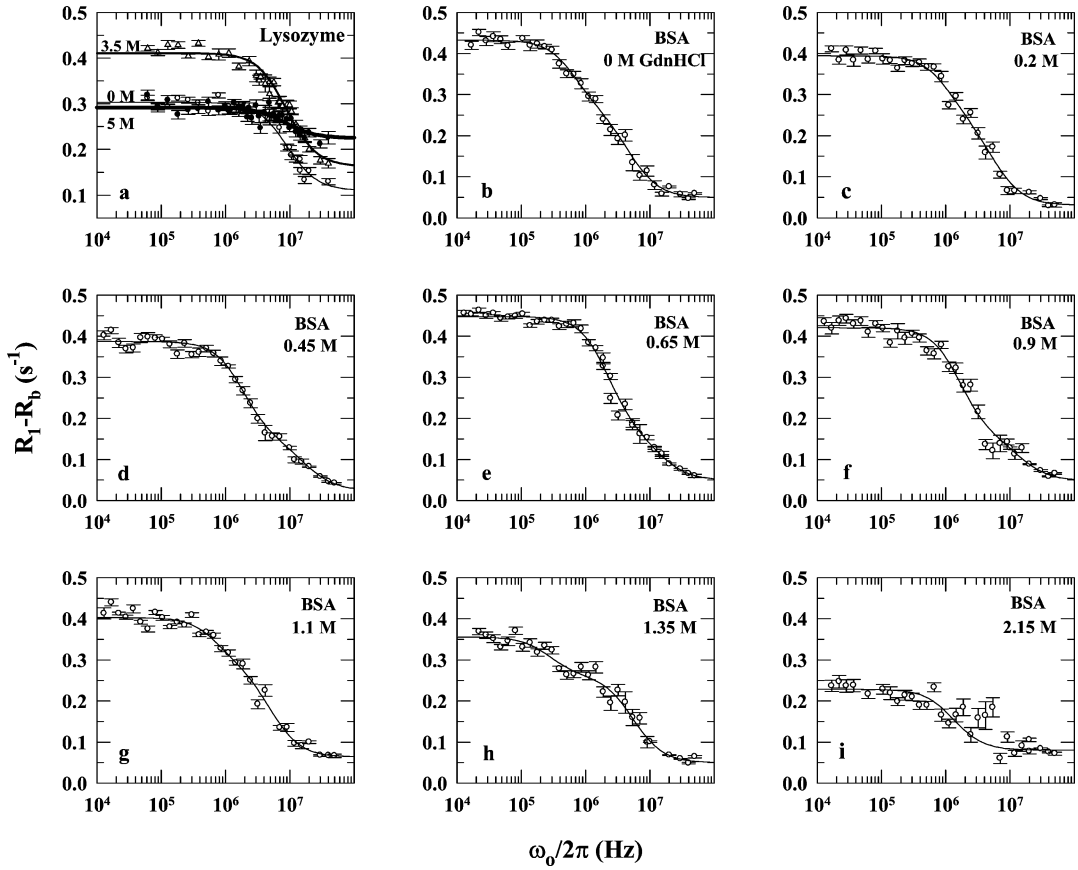

Figure 1. Water ^{1}H longitudinal relaxation dispersions for H_2O solutions of lysozyme (6 mM) and BSA (0.2 mM) at pH 4.4, 27 °C, in the presence of the GdnHCl concentrations indicated. (a) Representative dispersions showing the denaturant-induced changes in the dispersion of the lysozyme−water system. Solid lines represent three-parameter fits to data according to eq 1. The error bars were generated by repetitive measurements at the frequencies indicated. (b−i) Profiles for BSA illustrating stretched dispersions at the GdnHCl molarities indicated. The solid lines are multi-Lorentzian fits to the data according to eq 3. The fit parameters for all of the profiles are listed in Tables 1 and 3.

protein indicate constraints on the cavity water dynamics in the presence of subdenaturing amounts of GdnHCl.

2. Experimental Section

The commercial preparation of BSA (Sigma) was chromatographed on a Sephadex G75 column in 50 mM sodium phosphate buffer, pH 7, and the monomeric fraction obtained was dialyzed against deionized water. Hen egg white lysozyme from Calbiochem was used without further purification. GdnHCl was obtained from USB (Cleveland, OH). Protein samples were prepared in aqueous solutions of GdnHCl, and the pH was adjusted to 4.4 (electrode reading) by adding trace amounts of dilute HCl/NaOH. The pH remained constant in the entire duration of PMRD measurements. No attempt was made to remove dissolved oxygen, as the interest in the present studies was on the relative variation in the PMRD profiles as a function of denaturant concentration. The paramagnetic contribution to the relaxation due to the presence of dissolved oxygen was expected to be constant over the small variations in the concentration of GdnHCl used here. The concentration of GdnHCl was determined by refractive index measurements by the use of an Abbe-type refractometer.

2.1. Equilibrium Unfolding Measurements. Protein samples were prepared in the 0−6 M range of GdnHCl in 50 mM phosphate at pH 6.5 (BSA) or in water at pH 4.4 (lysozyme). The final protein concentrations were 5 μM for BSA and 2.2 μM for lysozyme. Samples were equilibrated at 27 °C for 7 h before recording fluorescence spectra. Emission spectra (excited at 280 nm, slit width: 0.75 nm) were taken in the 320−370 nm range setting the slit width to 1.25 nm. These measurements employed a photon counting instrument (FluoroMax-3, Jobin-Yvon, Horiba). The cell temperature was regulated at 27 (±0.5) °C by the use of a home-built external water circulation system.

2.2. PMRD Measurements. For ^{1}H relaxation dispersion measurements, 0.2 mM BSA monomer and 6 mM lysozyme samples were used. Measurements were performed using a commercial fast field cycling NMR (FFCNMR) spectrometer (Stelar, Italy) covering the frequency range of 10 kHz to 10 MHz and a home-built pulsed NMR spectrometer tunable in the 2−50 MHz frequency range. Conventional inversion/saturation recovery sequences were employed for measuring the longitudinal relaxation times on the pulsed NMR spectrometer. Nonpolarization and prepolarization sequences[30] were used for measurements on the FFCNMR spectrometer for the frequencies above and below 4 MHz, respectively. The temperature of the sample in the pulsed NMR spectrometer was regulated at 27 (±0.2) °C using a home-built gas-flow-type cryostat and a PID temperature controller. The FFCNMR spectrometer employs a VTC100 unit (Stelar, Italy) for this purpose, and the estimated stability in this case is within 0.5 °C.

3. Results and Analysis

3.1. Relaxation Dispersion. To investigate the effect of GdnHCl on protein hydration dynamics, ^{1}H relaxation in aqueous solutions of lysozyme and BSA containing the denaturant in the 0−5 M range was recorded. The effect is shown qualitatively in Figure 1 by a few representative profiles for

TABLE 1: Parameters Extracted from Fits of Lysozyme Relaxation Data to eq 1[a]

GdnHCl (M)	$R_b + \alpha$ (s^{-1})	β (10^7 s^{-2})	τ_c (10^{-8} s)
0	0.492	1.47	1.19
		(0.05)	(0.04)
0.65	0.489	1.52	1.25
		(0.07)	(0.13)
1.40	0.487	1.80	1.19
		(0.08)	(0.17)
1.9	0.488	1.61	1.13
		(0.04)	(0.03)
2.5	0.496	2.97	0.83
		(0.07)	(0.02)
3	0.505	2.40	0.98
		0.07	(0.03)
3.25	0.532	1.70	1.17
		(0.04)	(0.04)
3.5	0.554	2.34	1.05
		(0.05)	(0.03)
4	0.589	1.13	1.37
		(0.05)	(0.07)
5	0.657	0.61	1.07
		(0.06)	(0.12)

[a] Uncertainties in the parameter values are given within parentheses.

TABLE 2: Robustness of Analysis (F-Test to Fix the Number of Lorentzians in BSA Relaxation Data)

GdnHCl (M)	N	F	P
0	2	2.09	0.96
	3	0.10	0.45
0.2	2	1.54	0.81
	3	1.13	0.57
0.45	2	6.35	1.00
	3	0.94	0.36
0.65	2	2.83	1.00
	3	0.96	0.39
0.9	2	2.65	1.00
	3	0.94	0.36
1.1	2	1.67	0.87
	3	1.07	0.48
1.35	2	3.08	1.00
	3	0.97	0.39
1.8	2	1.40	0.75
	3	0.96	0.42
2.15	2	1.16	0.58

spin−lattice relaxation rate, R_1 ($=1/T_1$), as a function of resonance frequency, ω_o. Although the experimentally observed distribution is assumed to be a Lorentzian function of frequency, since the time-domain correlation function is generally exponential, the possibility of non-Lorentzian dispersion cannot be excluded. The denaturant dependency of the profile is typified by (i) the size of the relaxation amplitude across the range of ω_o employed and (ii) the characteristic details of the decrease in the relaxation rate in the fall-off region. The two criteria together define the dispersion step or the relaxation dispersion with frequency. Analyses of the curves provide important information about the effect of GdnHCl on the motion of the protein-bound water molecules and the correlation time for reorientation of the protein molecule.

3.2. Dispersion Profiles for Lysozyme. With initial increments of GdnHCl, the total change in R_1 of the lysozyme solution increases relative to that for native protein solution (Figure 1a). However, the size of the relaxation amplitude across ω_o is attenuated for increments beyond 3.5 M GdnHCl, as seen from the rather weak amplitude size for the sample containing 5 M GdnHCl. This qualitative assessment of dispersion plots indicates a nonlinear effect of GdnHCl concentration on lysozyme hydration dynamics: the total change in the relaxation amplitude initially increases and then decreases, displaying an inflection centered around 3.5 M GdnHCl. The inflection region for each profile ciphers some details of the protein motion, the critical frequency of reorientational motion notably, the extraction of which requires a detailed analysis. Considering the dispersions to be due to long-lived internal waters and labile hydrogens of the protein backbone,[14,31,32] the frequency dependence of the lysozyme relaxation rate was analyzed using a model described by

$$R_1 - R_b = \alpha + \beta\tau_c\left[\frac{0.2}{1+(\omega\tau_c)^2} + \frac{0.8}{1+(2\omega\tau_c)^2}\right] \quad (1)$$

Here, R_b represents the contribution to the relaxation from the bulk water molecules, and can be determined for aqueous solutions of GdnHCl by a single-frequency relaxation measurement (see below). α represents the contribution from the water molecules that are loosely bound to the protein surface. The second term on the right-hand side represents contributions from the integral water molecules buried inside the protein and the labile protons exchanging with the bulk water protons at a rate slow compared to the global correlation time associated with the isotropic tumbling of the protein, τ_c, but fast compared to the inherent relaxation rate of water. Under these conditions, the above model assumes that the integral waters and labile protons experience the same dynamics as the protein molecule. Since the dominant spin−spin interaction for protons in the type of systems under consideration is the dipolar interaction,[33] the parameter β includes the dipolar coupling constant (ω_D), the fraction of protons in integral water molecules and the labile protons in the total water molecules (f_I), and the generalized or orientational order parameter (S_I), which is included to take into consideration the averaging of the spin interaction by fast internal motions of the water molecules and labile protons. Thus, β is described by

$$\beta = \sum_\mu f_{I\mu}\omega_{D\mu}{}^2 S_{I\mu}{}^2 \quad (2)$$

Here, the summation is over different species of protons (integral waters and labile protons, for example) contributing to the relaxation dispersion. To obtain the parameters $R_{1b} + \alpha$, β, and τ_c, the relaxation dispersion data for each concentration of GdnHCl were fitted to eq 1 using a nonlinear least-squares procedure based on the Levenberg−Marquardt algorithm. The continuous lines through the dispersion data for lysozyme (Figure 1a) are fits to the equation. The fit parameters extracted for all concentrations of GdnHCl are listed in Table 1.

3.3. Dispersion Profiles for BSA. The BSA data are relatively complex, and the spectral density function changes with GdnHCl increments in an involved manner (Figure 1b−i). The dispersions will have contributions form various other possible mechanisms, as listed below, apart from the isotropic tumbling of the protein molecules. Earlier PMRD studies on BSA also showed signatures of non-Loretzian dispersions.[29] These stretched dispersions may have various interpretations based on some form of correlation time distribution.[14] Apparently non-Lorentzian frequency distribution of R_1 could arise from a number of factors including complex reorientational dynamics due to structural heterogeneity, a distribution of proton exchange rates for buried water molecules and labile protein protons, aggregation, and a distribution of intermolecular dipole couplings. Unlike lysozyme, BSA is a multidomain protein and

TABLE 3: Parameters Extracted from the Model Free Analysis of BSA Relaxation Data[a]

GdnHCl (M)	α (s^{-1})	β_1 (10^7 s^{-2})	β_2 (10^7 s^{-2})	τ_{c1} (ns)	τ_{c2} (ns)	β (10^7 s^{-2})	$\langle\tau_c\rangle$ (ns)
0	0.412	0.14	1.12	128.75	18.31	1.26	30.38
	(0.001)	(0.03)	(0.07)	(15.55)	(1.89)	(0.1)	(2.54)
0.2	0.394	0.21	1.27	79.03	15.67	1.48	24.55
	(0.002)	(0.07)	(0.08)	(13.60)	(2.14)	(0.15)	(1.56)
0.45	0.389	0.52	2.36	46.84	4.99	2.88	12.57
	(0.003)	(0.04)	(0.18)	(2.47)	(0.53)	(0.22)	(0.77)
0.65	0.414	0.75	1.72	39.25	6.03	2.47	16.11
	(0.003)	(0.08)	(0.16)	(2.22)	(1.08)	(0.24)	(0.76)
0.9	0.414	0.51	1.68	53.09	6.10	2.18	17.02
	(0.002)	(0.05)	(0.12)	(3.84)	(0.84)	(0.17)	(0.70)
1.1	0.430	0.11	1.25	114.93	17.34	1.35	25.05
	(0.001)	(0.02)	(0.06)	(13.83)	(1.41)	(0.08)	(3.29)
1.35	0.418	0.03	1.28	318.75	16.31	1.31	23.32
	(0.001)	(0.01)	(0.05)	(49.42)	(0.76)	(0.06)	(0.84)
1.8	0.451	0.11	0.64	271.97	20.61	0.75	56.94
	(0.001)	(0.01)	(0.06)	(20.31)	(2.78)	(0.07)	(12.60)
2.15	0.451	0.22		67.98		0.20	67.98
	(0.001)	(0.02)		(6.67)		(0.02)	(6.67)

[a] Uncertainties in parameter values are given within parentheses.

is structurally more complex. The analyses of the dispersion profiles therefore seemed nontrivial. It has been emphasized, though, that a model-free approach for analyzing such stretched dispersion profiles produces parameters with well-defined physical significance.[14] We therefore fitted the BSA data to the multi-Lorentzian equation

$$R_1 - R_b = \alpha + \sum_N \beta_N \tau_{cN} \left[\frac{0.2}{1 + (\omega\tau_{cN})^2} + \frac{0.8}{1 + (2\omega\tau_{cN})^2} \right] \quad (3)$$

where R_b, α, and β have meanings as described earlier for the analysis of lysozyme data (eq 1). The number N of the Lorentzians to be included here was objectively determined by means of the F-test starting with $N = 1$ and successively adding terms until the probability $P(N+1) < P_0$, where the probability cutoff P_0 was taken as 0.8. Table 2 shows the robustness of the analysis, and the fits through the dispersion data are shown by the continuous lines in Figure 1b−i. The dispersion amplitude β and the average correlation time $\langle\tau_c\rangle$ were calculated by

$$\beta = \sum_N \beta_N \quad \text{and} \quad \langle\tau_c\rangle = \frac{\sum_N \beta_N \tau_N}{\sum_N \beta_N} \quad (4)$$

The parameters extracted from these analyses are listed in Table 3.

3.4. Response of α with GdnHCl. The parameter α represents the contribution of a sizable set of water molecules at the protein surface to the experimentally observed R_1 of the protein−solvent system. In protein folding studies, the response of α with the denaturant can therefore provide information about the action of the denaturant on the surface area, surface occupancy by water, and the corresponding hydration dynamics. In principle, the high-frequency plateau in the dispersion profile provides the value of R_b + α. However, since R_b can be determined trivially by a single-frequency longitudinal relaxation measurement, the response of α with increments of the denaturant can be closely examined. In this study, the GdnHCl dependence of R_b was measured at 50 MHz (Figure 2a). The data do not indicate any significant change in the relaxation rate of bulk water in the presence of a subdenaturing or low concentration of GdnHCl (<3 M), suggesting that the rotational correlation time of water molecules is unaltered, or increases slightly at the most. The marginal increase observed in Figure 2a is due to the contribution of GdnHCl to the bulk viscosity determined as described earlier.[34] We nevertheless take this viscosity increase to be insignificant. In aqueous solutions, low concentrations of urea have been shown to reduce the extent of water hydrogen bonding.[1] Whether such effects of denaturants on bulk water are related to the protein folding process, and to what extent, if yes, is open to investigation.

The variation of α with GdnHCl is illustrated for the lysozyme and BSA systems in Figure 2b,c. The correlation time associated with the dynamics of the surface waters, τ_{cS}, is very short, resulting in extreme narrowing condition for the Larmor frequencies used here (i.e., $\omega\tau_{cS} \ll 1$). Figure 2b,c also shows the expected variation of α with the change in the viscosity of the solvent due to the presence of the denaturant computed by assuming that the variation in α is mainly due to the variation in the corresponding correlation time for exchange with the bulk water, which in turn is proportional to viscosity.[35] The experimental and calculated distributions are not closely comparable; the former varies initially slower than expected. At low concentrations of GdnHCl, the value of α is reduced (for BSA) or stays constant (for lysozyme), but at higher concentrations of the denaturant, the global structure unfolding effect leads to a rapid rise in the value of α. Three other parameters influence the value of α: (i) the solvent accessible surface area of the protein, (ii) the relative occupancy of water and denaturant molecules at the protein surface, and (iii) the rotational dynamics of the persistent water molecules at the protein surface. The presence of GdnHCl can affect any and all of these factors. For example, the protein could possibly shrink before any major unfolding event, and that will reduce surface hydration, leading to the initial modest variation of α. Even more, any or all three factors could be responsible for the observed response of α with GdnHCl. Therefore, we refrain from providing a unique interpretation for the experimental behavior of α. The results, however, emphasize the fact that apart from the effect on intrinsic protein structure and segmental dynamics, as are commonly considered for a mechanistic description of protein folding, low concentrations of GdnHCl can have a considerable influence on the surface hydration.

3.5. Response of β with GdnHCl. As mentioned earlier, the parameter β includes the dipolar coupling constant (ω_D), the

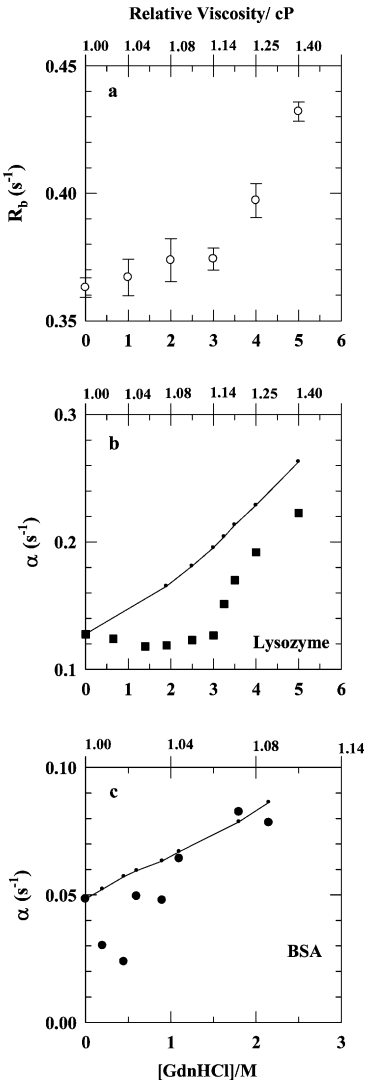

Figure 2. (a) Effect of GdnHCl on the ^{1}H longitudinal relaxation rate constant for bulk water R_b measured at 50 MHz, 27 °C. The variation is not quite considerable in the subdenaturing limit of the denaturant concentration. The GdnHCl dependency of α that represents the contribution of the protein surface waters to the observed relaxation rate constant for the lysozyme−H_2O and BSA−H_2O systems is shown in panels b and c, respectively. The symbols represent the values extracted from fits of the dispersion data to eq 1 (for lysozyme) and eq 3 (for BSA). The solid lines represent the expected variation of α with the change in the viscosity of the protein solution due to added GdnHCl as described in the text.

fraction of protons in integral water molecules and the labile protons in the total water molecules (f_I), and the generalized or orientational order parameter (S_I). Figure 3 shows the variation of β as a function of GdnHCl. Interestingly, with increments of the denaturant concentration, β initially increases and then decreases for both lysozyme and BSA systems (Figure 3a,b). Insufficiently defined high-frequency plateaus of the dispersion curves can make the Lorentzian fits sensitive to random or data error. In the present experiments, data were recorded up to 40 MHz for lysozyme and 50 MHz for BSA, and we do not believe that the high-frequency plateau is so ill-defined that the error in values of β would overwhelmingly show up in the observed variation of β with GdnHCl. The feature in the variation of β is observed for both proteins, and the GdnHCl concentration corresponding to the maximum value of β lies in the pretransition region of the equilibrium unfolding curve (see below). The accentuated decrease in the value of β (>2.5 M GdnHCl

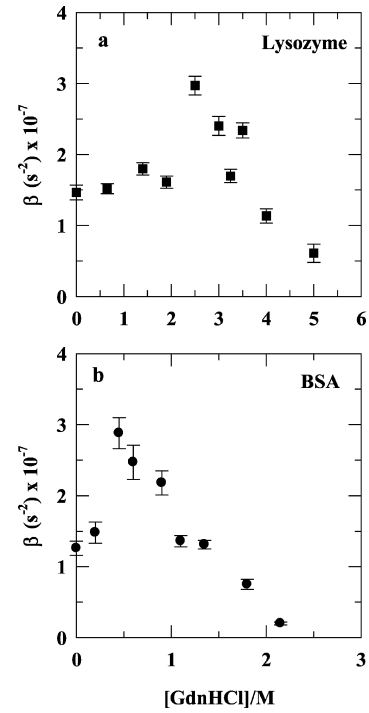

Figure 3. Variation of β with increments of GdnHCl illustrated for (a) lysozyme and (b) BSA. The values of β were obtained from the Lorentzian fits as described in the text.

for lysozyme and >0.5 M GdnHCl for BSA) is due to the unfolding effect of the denaturant. Unfolding of the tertiary structure leads to a reduction in the number of long-lived internal waters and hence a gradual loss in the dispersion amplitude.[17] However, the initial rise in the value of β in the subdenaturing or moderately denaturing region is certainly not due to an increase in the number of internal waters. As no major structural changes are expected to occur in the proteins at such low concentrations of GdnHCl, neither the f_I's nor ω_D's are expected to vary. Therefore, we attribute the observed change in β largely to the variation in S_I, implying that the order parameter increases in the presence of low concentrations of GdnHCl. Also to note, at the experimental pH of 4.4 employed here, where the labile hydrogens are expected to exchange very slowly, their contribution to the relaxation dispersion may not be significant.

3.6. Response of τ_c with GdnHCl. In the formal parametrization of dispersion profiles, the dispersion amplitude is represented by $\beta\tau_c$, where τ_c is the effective correlation time, whose value is extracted from the fit of the data to eq 1. Since the rotational correlation time of the protein τ_R is generally much shorter than the residence times of the internal water molecules that contribute to the dispersion, the effective correlation time can be equated with τ_R according to the equation

$$\frac{1}{\tau_c} = \frac{1}{\tau_W} + \frac{1}{\tau_R} \tag{5}$$

where τ_W is the residence time of the integral waters in the protein. The formalism and the validity of this assumption have been discussed earlier.[14] Values of τ_c can be calculated from

$$\tau_c \approx \tau_R = \frac{\eta V}{k_B T} \tag{6}$$

where η is the viscosity of the water−protein−GdnHCl system and V is the hydrodynamic volume of the protein.

Figure 4 shows the experimentally obtained and estimated values of τ_c for lysozyme and BSA as a function of GdnHCl.

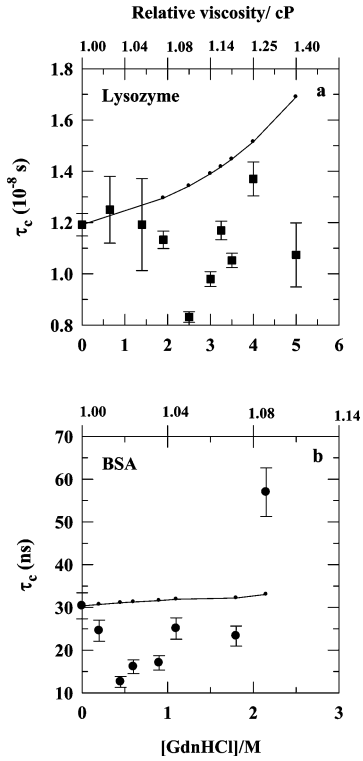

Figure 4. Response of the effective correlation time τ_c to the molarity of GdnHCl shown for lysozyme (a) and BSA (b). The solid lines, calculated by using the Debye−Stokes−Einstein relation (eq 5), estimate the expected behavior where the hydrodynamic volumes (V) of the proteins are assumed not to vary significantly.

The correlation time of lysozyme in the absence of denaturant obtained here is 11.9 ± 0.4 ns, slightly higher than the values of 8.7 ± 1.3 and 9.0 ± 0.2 ns reported earlier.[36,37] The average correlation time for BSA at 0 M denaturant is 30 ± 3 ns, less than the published values of 41 ± 3 ns in H_2O and 51 ± 4 ns in D_2O.[24] To note, a value of 49 ± 2 ns is obtained in our study also when a single Lorentzian is used to fit the BSA data. However, as discussed above, the complexity of BSA dispersion profiles warrants multi-Lorentzian fits of the data. For estimation of values of τ_c, we have assumed that V does not change within the range of the denaturant employed here. For both proteins, the experimentally derived τ_c decreases with initial increments of the denaturant, and the GdnHCl concentration for the τ_c minimum corresponds to the respective GdnHCl concentration at which β is maximum (Figure 3). Clearly, the experimental data are inconsistent with the $\tau_c \approx \tau_R =$ constant $\times \eta$, suggesting a slight shrinkage in hydrodynamic volumes of the proteins under subdenaturing conditions.

3.7. Equilibrium Unfolding of Lysozyme and BSA. To relate the observed variation in the values of β and τ_c to the structure and dynamics of the proteins, we measured their GdnHCl-induced equilibrium unfolding transitions by fluorescence (Figure 5). In the primary data, the pretransition region for both proteins is marked by some positive slope (Figure 5a,c). The feature observed here for BSA is consistent with data published earlier,[26] and the analyses employed could be subjective with reference to involvement of equilibrium intermediates. For the present purpose, though, we calculated the fraction folded for each protein, and fitted the data to the two-state equation:[38]

$$S_{obs} = \frac{(c_f + m_f[D]) + (c_u + m_u[D]) \exp\left[\frac{-\Delta G_D^\circ + m_g[D]}{RT}\right]}{1 + \exp\left[\frac{-\Delta G_D^\circ + m_g[D]}{RT}\right]} \quad (7)$$

where S_{obs} is the observed emission signal, c_f and c_u and m_f and m_u represent intercepts and slopes of native and unfolded baselines, respectively, ΔG_D° is the free energy of unfolding, [D] is the denaturant concentration, and m_g represents the change in surface area during global unfolding of the protein. Again, a two-state analysis, especially for BSA, may not be uncontestable, but the purpose here is to map the observed features of β and τ_c onto the equilibrium melting transition. The thermodynamic parameters obtained from the fits are given in the legend to Figure 5. The data show large-scale global transition setting in beyond ~3 M GdnHCl for lysozyme and ~1.5 M GdnHCl for BSA. This is consistent with the drop in β values at denaturant concentrations >3 M for lysozyme and >1 M for BSA (Figure 5b,d). Under subdenaturing conditions, the β value increases due to an increase in the orientational order parameter of internal waters, and the τ_c value decreases due possibly to a shrinkage in the hydrodynamic volume of the protein.

4. Discussion

This study examines the effect of GdnHCl on hydration dynamics of lysozyme and BSA by the use of ^{1}H magnetic relaxation dispersion which unlike the other commonly used spectroscopic probes reports on changes in the water molecules that bind to the protein for times long compared with the rotational correlation time of the protein. The key observations emerging from the analyses of the dispersion data are (i) a distinctly biphasic variation of the magnitude of the parameter β apparent by an initial rise in the subdenaturing limit followed by a sharp drop as unfolding conditions are approached and

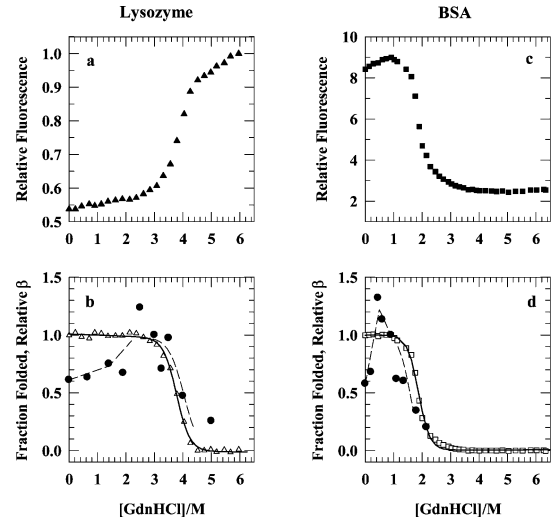

Figure 5. GdnHCl-induced equilibrium unfolding of lysozyme (a, b) and BSA (c, d), monitored by tryptophan fluorescence. (b, d) The unfolding data normalized as fraction folded is compared with the variation of β. For the purpose of the comparison, the denaturant dependence of the β value has been arbitrarily scaled down. The continuous lines through the normalized data (b, d) represent least-squares fits using a two-state model according to eq 6. Values of ΔG_D° and m_g are 9.3 (±0.1) kcal mol^{-1} and 2.4 (±0.1) kcal mol^{-1} M^{-1}, respectively, for lysozyme and 5.6 (±0.32) kcal mol^{-1} and 3.0 (±0.15) kcal mol^{-1} M^{-1}, respectively, for BSA. The broken lines through the β values have been drawn by inspection only.

(ii) a slight plunge in the hydrodynamic volume in the subdenaturing limit, followed by its recovery and rise at higher concentrations of the denaturant.

4.1. The Order Parameter of Integral Waters May Increase due to Denaturant-Induced Protein Stiffening. The parameter β exhibits a nonlinear dependence on GdnHCl (Figure 3). We have reasoned above that the observed response of β is due to an increase in the order parameter S_I of integral waters when subdenaturing amounts of GdnHCl are included in the protein solution. With further increments of GdnHCl, the decrease of S_I is evidently due to protein denaturation and gradual unfolding with concomitant loss of structure. Central to the integral water-ordering effect of subdenaturing amounts of denaturant is the mode of action of denaturants on proteins. Although the protein unfolding effect of denaturants can be completely described along thermodynamic lines, models that consider protein−denaturant binding are also equally successful and sufficient to describe the unfolding process,[39] and in fact, consideration of such interactions can provide clues to the structural mechanism and motional processes that govern protein folding. Binding of chemical denaturants to proteins has now been unequivocally established using X-ray crystallography and calorimetric studies of protein−denaturant systems. Crystal structures of several proteins, including α-chymotrypsinogen,[40] lysozyme,[41−43] and DHFR and RNASe A,[44] with urea and GdnHCl have provided evidence that the denaturant molecules directly interact with protein side chain and main chain atoms by multiple hydrogen-bonding interactions of variable length as well as by van der Waals interactions.[44] Calorimetric study has indicated that, in the presence of 3 M GdnHCl, where the maximum of β is seen here (Figure 3a), roughly 13 molecules of GdnHCl will bind to one molecule of lysozyme.[45] For BSA, the crystal structure has not been made available, and detailed calorimetric study has not been done. However, it is clear that $GdnH^+$ ions will bind to BSA as well.

An important outcome of denaturant binding under subdenaturing conditions is that the protein is dynamically constrained especially in those parts that harbor the GdnHCl binding sites. Multiple hydrogen-bonding and van der Waals interactions by which a $GdnH^+$ ion can interact with several atoms from residues in spatial proximity can serve to cross-link parts of the protein molecule. As a consequence, the internal motions at the sites of the affected residues will be constrained. In fact, X-ray data on lysozyme and other proteins in the presence of denaturants do show a considerable reduction in the B-factor for side chains and main chain atoms.[41] Manifests of the dynamic constraints include a decrease in the native-state fluctuations in the positions of individual or clusters of atoms around their average, and an increase in the barrier to motion in the more compact conformer of the protein, and hence a reduction in the rate of subglobal unfolding motions.[46]

These facts provide a basis for understanding the behavior of β with GdnHCl (Figure 3). The protein stiffening effect of subdenaturing concentrations of GdnHCl can be inductively conveyed to the cavity waters, since these water molecules can interact directly with the backbone and side chains in the protein interior.[9] Even if the internal waters make no contact with the protein chain, the stiffened protein can constrain them indirectly, through a decrease in the volumes of internal cavities, for example. Thus, the increase in the dispersion amplitude in the presence of lower concentrations of the denaturant must originate largely from changes in dynamics of the internal cavity waters. These dynamics, considered under the generalized order parameter, S_I, include reorientational motions of the water molecules that are fast relative to the isotropic global tumbling of the protein. Libration amplitudes of cavity waters have been described within the formalism of the anisotropic harmonic libration (AHL) model.[14,47] For ^1H, the generalized order parameter S_I is affected by rocking and twisting motions of the water.[14] We thus suggest that in the presence of lower concentrations of GdnHCl it is the higher S_I for one or more cavity waters that dominates, and consequently the value of β increases (Figures 3 and 5). Under strongly unfolding conditions, achieved with further increments of GdnHCl, the structure-ordering effect of the denaturant is overwhelmed by its own structure-unfolding effect. The disappearance of water cavities is now reflected in the drop of β (Figure 3).

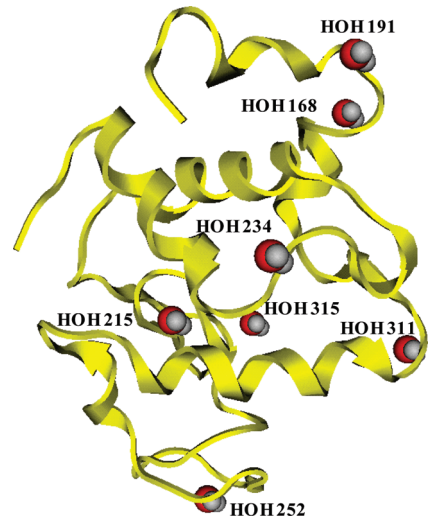

Figure 6. Ribbon diagram of lysozyme showing the crystallographically defined buried waters. In the presence of subdenaturing amounts of urea, the water HOH 191 interacts directly with a urea molecule.

It should be mentioned that the denaturant molecules can also promote the order of cavity waters directly by interacting with them. For instance, the crystal structures of lysozyme with a subdenaturing amount of urea clearly show one of the seven internal waters, HOH 191 (Figure 6), directly interacting with a urea molecule, urea 256, through a pair of hydrogen bonds.[41] Involvement of internal water molecules in the interaction of GdnHCl (1.2 M) with lysozyme was not noticed, though.[43] In spite of this, the influence of $GdnH^+$ ions on the cavity waters cannot be ruled out.

We also note that a similar trend in the variation of β, as shown here for lysozyme and BSA (Figures 3 and 5), has been reported earlier for a β-barrel protein, namely, intenstinal fatty acid binding protein.[17] Although the data were interpreted in terms of accumulation of an equilibrium folding intermediate, the authors have mentioned the possibility of trapping of one or two previously short-lived water molecules by urea molecules in long-lived association with the protein.[17] We suggest it is the effect of the denaturant on S_I rather than the accumulation of folding intermediates that is reflected by the data. Lysozyme is one of most well studied proteins, and there is no evidence for the accumulation of a folding intermediate at equilibrium. A similar pattern of variation of β with GdnHCl observed for other protein systems (unpublished results) provides a basis for the suggestion that denaturant-mediated intramolecular protein cross-linking generally encourages cavity water order.

The pretransition baselines of equilibrium unfolding transitions of proteins hardly convey any information about the structural and dynamical transitions in the subdenaturing limit of denaturants. In general, slopes and curvatures in the pretran-

sition baselines, as seen here for lysozyme and BSA (Figure 5a,c), are taken to originate from protein−solvent interactions, and the global structural unfolding transition is fit to a two- or three-state model by assuming a linear or polynomial dependence of the spectroscopic observable on the denaturant concentration. It is, however, clear that strategic experiments, including measurements of T_1, T_2, and heteronuclear $\{^1H\}-^{15}N$ NOEs on ^{15}N-labeled proteins, are warranted to understand the influence of low concentrations of denaturants on proteins, and such data are crucial to understanding not only the mechanism of protein folding but also the structural and dynamical factors contributing to protein stability. With the results available here, the changes in the baseline regions for lysozyme and BSA can be related to constraints on protein structure and motions. However, the occurrence of these changes in the state of a protein cannot be ruled out even when the baseline is flat. In other words, the observed spectroscopic changes in the baseline region do not serve as markers.

4.2. Thermodynamic Consequences of GdnHCl-Induced Motional Constraints on the Protein. How do protein−GdnHCl interactions in the subdenaturing limit affect protein stability? The enthalpy of transformation of the native protein state to a near-native state by low concentrations of GdnHCl is likely to be negative (ΔH is −ve) due to additional hydrogen-bonding interactions experienced by the protein. However, the motional constraints imposed by denaturant binding are expected to reduce the entropy of various origins, including local entropy due to atomic fluctuations and side chain rotations. Consequently, the transition of the native state to a near-native or subdenatured state should be entropically disfavored (ΔS is −ve). These expectations do not allow drawing a definite conclusion about the energetic stability of a near-native state relative to the native state in aqueous solution. Whether such a subdenatured state is more stable than the native state (ΔG is −ve) depends on the magnitudes of ΔH and ΔS. It should also be clear that the magnitude of ΔH will depend on the abundance and importance of interactions other than hydrogen bonding in the subdenatured state produced by protein−GdnHCl interactions.

In fact, investigations from time to time have provided evidence that subdenaturing concentrations of GdnHCl stabilize proteins.[1−5] In such studies reported earlier, GdnHCl has been thought to affect the stability electrostatically by virtue of its ionic nature. Just as Cl^- ion can stabilize proteins by electrostatic effects, through Debye−Hückel charge screening, for example, $GdnH^+$ ion can also be stabilizing due to its interaction with specific cation binding sites on the protein.[3] The stabilization of the acid molten globule state of proteins by low concentrations of GdnHCl, due to binding of Cl^- to the cationic sites,[6,7] provides a classic example of electrostatic stabilization. Solutes such as NaCl and Na_2SO_4 stabilize proteins by the same mechanism involving an ion pair type or charge screening type of interactions. The electrostatic mechanism, however, tends to overlook the thermodynamic consequences of denaturant binding to proteins. The thermodynamic view cannot be overlooked simply because the nonionic denaturant urea that interacts with proteins in a manner nearly identical to that of GdnHCl has also been found to stabilize proteins. Clearly then, urea-induced protein stabilization must rest solely on thermodynamic consequences of denaturant binding. We have posited that subdenaturing amount of denaturants could stabilize proteins despite the decreased entropy presumably by a compensatory role of enthalpy.[46,48,49] Such stabilization may add onto the global stability or could be manifested at a subglobal level, perhaps depending on the extent and distribution of protein−denaturant interactions and denaturant-mediated intraprotein cross-links.[46] From these considerations, it appears that subdenaturing concentrations of GdnHCl facilitate access of lysozyme and BSA to more stable states in the respective free energy landscapes. Although the extent of stabilization and whether at a global or subglobal level can be investigated by classical equilibrium unfolding experiments using pH, temperature, and denaturants as variables, we have not delved into such details in the present study. Also, segregation of the electrostatic and entropic effects on the hydration dynamics of these proteins warrants further studies of NMR relaxation dispersion in the presence of salt and urea.

4.3. Hydrodynamic Volume under Subdenaturing Conditions. The small shrinkage of the hydrodynamic volumes for the two proteins under subdenaturing conditions (Figure 4) is intriguing because dynamic light scattering data do not show such nonlinearity in the pretransition region of the unfolding transition. The nature of modulation of the surface water density by GdnHCl could shed some light. Unfortunately, enthusiasm in this direction is marred by complications arising from the solvent-dependent partial specific volume of protein,[6] but this aspect of protein dynamics certainly deserves more attention. The role of surface waters in protein folding has not been experimentally investigated to any detail. The simulation-based desolvation model for the kinetics of folding (U → N, where U and N are unfolded and native states) posits that squeezing out some of the surface waters is necessary for a collapsed protein to achieve the native folded state.[7] This drying effect that decreases the surface water density appears to suppress protein flexibility significantly,[50,51] apart from causing a reduction in the water−protein electrostatic forces.[52] In this perspective, a small decrease in the hydrodynamic volume can possibly be attributed to the intramolecular protein cross-linking and stiffening effect of GdnHCl discussed above. The observed variation of τ_c should mean some global shrinkage resulting in a more compact molecule with a relatively water-stripped surface and reduced hydrodynamic volume. At present, we do not have data to expound further on this mechanism.

Summary and Conclusion

Stoichiometric binding theory for direct protein−denaturant interaction affords a satisfactory interpretation of protein unfolding transitions.[39,53] However, the effect of lower concentrations of denaturants on structure and dynamics of proteins has received meager attention. The present work reveals nonlinear modulation of hydration dynamics of lysozyme and BSA by GdnHCl. The dispersion amplitude of ^1H relaxation in protein solutions is proven to be sensitive enough to detect the denaturant-induced changes in the dynamics of the protein-bound waters having long residence times compared with the rotational correlation time of the protein.

Acknowledgment. This work was supported by grants from the Inter University Consortium, India (IUC/AO/MUM/CRS-M-110/03/288), and DBT (BRB/15/227/2001).

References and Notes

(1) Finer, E. G.; Franks, F.; Tait, M. J. *J. Am. Chem. Soc.* **1972**, *94*, 4424.

(2) Eisenberg, D.; Kauzmann, W. *The Structure and Properties of Water*; Oxford University Press: New York, 1969.

(3) Soper, A. K.; Castner, E. W.; Luzar, A. *Biophys. Chem.* **2003**, *105*, 649.

(4) Kamal, J. K. A.; Zhao, L.; Zewail, A. H. *Proc. Natl. Acad. Sci. U.S.A.* **2004**, *101*, 13411.

(5) Pal, S. K.; Peon, J.; Zewail, A. H. *Proc. Natl. Acad. Sci. U.S.A.* **2002**, *99*, 15297.
(6) Svergun, D. J.; Richard, S.; Koch, M. H.; Sayers, Z.; Kuprin, S.; Zaccai, G. *Proc. Natl. Acad. Sci. U.S.A.* **1998**, *95*, 2267.
(7) Levy, Y.; Onuchic, J. N. *Annu. Rev. Biophys. Biomol. Struct.* **2006**, *35*, 389.
(8) Meyer, E. *Protein Sci.* **1992**, *1*, 1543.
(9) Park, S.; Saven, J. G. *Proteins: Struct., Funct., Bioinf.* **2005**, *60*, 450.
(10) Otting, G.; Liepinsh, E.; Wuthrich, K. *Science* **1991**, *254*, 974.
(11) Denisov, V. P.; Halle, B. *J. Mol. Biol.* **1995**, *245*, 682.
(12) Garcia, A. E.; Hummer, G. *Proteins: Struct., Funct., Genet.* **2000**, *38*, 261.
(13) Denisov, V. P.; Halle, B. *Faraday Discuss.* **1996**, *103*, 227.
(14) Halle, B.; Denisov, V. P.; Venu, K. In *Biological Magnetic Resonance*; Krishna, N. R., Berliner, L. J., Eds.; Kluwer Academic/Plenum Publishers: New York, 1999; p 419.
(15) Persson, E.; Halle, B. *J. Am. Chem. Soc.* **2008**, *130*, 1774.
(16) Denisov, V. P.; Jonsson, B.; Halle, B. *Nat. Struct. Biol.* **1999**, *6*, 253.
(17) Modig, K.; Kurian, E.; Prendergast, F. G.; Halle, B. *Protein Sci.* **2003**, *12*, 2768.
(18) Evans, P. A.; Topping, K. D.; Woolfson, D. N.; Dobson, C. M. *Proteins: Struct., Funct., Genet.* **1991**, *9*, 248.
(19) Morozova, L. A.; Haynie, D. T.; Arico-Muendel, C.; Van Dael, H.; Dobson, C. M. *Nat. Struct. Biol.* **1995**, *2*, 871.
(20) Knubovets, T.; Osterhout, J. J.; Connolly, P. J.; Klibanov, A. M. *Proc. Natl. Acad. Sci. U.S.A.* **1999**, *96*, 1262.
(21) Tanford, C.; Aune, K. C.; Ikai, A. *J. Mol. Biol.* **1973**, *73*, 185.
(22) Kuwajima, K.; Hiraoka, Y.; Ikeguchi, M.; Sugai, S. *Biochemistry* **1985**, *24*, 874.
(23) Radford, S. E.; Dobson, C. M.; Evans, P. A. *Nature (London)* **1992**, *358*, 302.
(24) Wildegger, G.; Kiefahber, T. *J. Mol. Biol.* **1997**, *270*, 294.
(25) El Kadi, N.; Taulier, N.; Le Huerou, J. Y.; Gindre, M.; Urbach, W.; Nwigwe, I.; Kahn, P. C.; Waks, M. *Biophys. J.* **2006**, *91*, 3397.
(26) Ahmad, B.; Kamal, M. Z.; Khan, R. H. *Protein Pept. Lett.* **2004**, *11*, 307.
(27) Efimova, Y. M.; Haemers, S.; Wierczinski, B.; Norde, W.; van Well, A. A. *Biopolymers* **2007**, *85*, 264.
(28) Denisov, V. P.; Peters, J.; Hörlein, H. D.; Halle, B. *Nat. Struct. Biol.* **1996**, *3*, 505.
(29) Kiihne, S.; Bryant, R. G. *Biophys. J.* **2000**, *78*, 2163.
(30) Anoardo, E.; Galli, G.; Ferrante, G. *Appl. Magn. Reson.* **2001**, *20*, 365.
(31) Halle, B.; Denisov, V. P. *Methods Enzymol.* **2001**, *338*, 178.
(32) Venu, K.; Denisov, V. P.; Halle, B. *J. Am. Chem. Soc.* **1997**, *119*, 3122.
(33) Abragam, A. *The Principles of Nuclear Magnetism*; Clarendon Press: Oxford, U.K., 1961.
(34) Rao, D. K.; Bhuyan, A. K. *J. Biomol. NMR* **2007**, *39*, 187.
(35) Cantor, R. C.; Schimmel, P. R. *Biophysical Chemistry*; W. H. Freeman and Company: New York, 1980; Vol. II, p 461.
(36) Gottschalk, M.; Halle, B. *J. Phys. Chem. B* **2003**, *107*, 7914.
(37) Luchinat, C.; Parigi, G. *J. Am. Chem. Soc.* **2007**, *129*, 1055.
(38) Santoro, M. M.; Bolen, D. W. *Biochemistry* **1988**, *27*, 8063.
(39) Schellman, J. A. *Biopolymers* **1978**, *17*, 1305.
(40) Hibbard, L. S.; Tulinsky, A. *Biochemistry* **1978**, *17*, 5460.
(41) Pike, A. C. W.; Acharya, R. *Protein Sci.* **1994**, *3*, 706.
(42) Snape, K. W.; Tjian, R.; Blake, C. C. F.; Koshland, D. E. *Nature (London)* **1974**, *250*, 295.
(43) Mande, S. C.; Sobhia, M. E. *Protein Eng.* **2000**, *13*, 133.
(44) Dunbar, J.; Yennawar, H. P.; Banerjee, S.; Luo, J.; Farber, G. K. *Protein Sci.* **1997**, *6*, 1272.
(45) Makhatadze, G. I.; Privalov, P. L. *J. Mol. Biol.* **1992**, *226*, 491.
(46) Bhuyan, A. K. *Biochemistry* **2002**, *41*, 13386.
(47) Denisov, V. P.; Venu, K.; Peters, J.; Hörlein, H. D.; Halle, B. *J. Phys. Chem. B* **1997**, *101*, 9380.
(48) Kumar, R.; Prabhu, N. P.; Yadaiah, M.; Bhuyan, A. K. *Biophys. J.* **2004**, *87*, 2656.
(49) Kumar, R.; Bhuyan, A. K. *J. Biol. Inorg. Chem.* **2009**, *14*, 11.
(50) Huang, Q.; Ding, S. W.; Hua, C. Y.; Yang, H. C.; Chen, C. L. *J. Chem. Phys.* **2004**, *121*, 1969.
(51) Liu, P.; Huang, X.; Zhou, R.; Berne, B. J. *Nature (London)* **2005**, *437*, 159.
(52) Zhou, R. H.; Huang, X. H.; Margulis, C. J.; Berne, B. J. *Science* **2004**, *305*, 1605.
(53) Schellman, J. A. *Annu. Rev. Biophys. Biophys. Chem.* **1987**, *16*, 115.

JP8114836